Structure and phase equilibria of the soybean lecithin/ PEG 40 Monostearate/ water system

Montalvo, G.[1,†,]*, Pons, R.*[2]*; Zhang, G.*[3‡]*; Díaz, M.*[4]*; Valiente, M.*[1]

1 Departamento de Química Analítica, Química Física e Ingeniería Química. Universidad de Alcalá. E28871 Alcalá de Henares (Madrid), Spain.

2 Department de Tecnologia Química i de Tensioactius, IQAC-CSIC, E08034 Barcelona, Spain.

3 Leiden Institute of Chemistry, 2300 RA Leiden, Netherland.

4 Facultad Seccional Sogamoso- Ingeniería Geológica, Universidad Pedagógica y Tecnológica de Colombia, Calle 4 Sur No.15 -134 Sogamoso-Boyacá-Colombia.

† Instituto Universitario en Ciencias Policiales (IUICP), Ctra. Madrid-Barcelona Km. 33.600, 28871 Alcalá de Henares (Madrid), Spain.

KEYWORDS

Lecithin, PEG 40 monostearate, phase behavior, differential scanning calorimetry (DSC), optical microscopy, small-angle X-ray scattering (SAXS), rheology.

ABSTRACT

PEG stearates are extensively used as emulsifiers in many lipid-based formulations. However, the scheme of the principles of the lipid-surfactant polymer interactions are still poorly understood and need more studies. A new phase diagram of lecithin/ PEG 40 monostearate/ water system at 30 ºC is reported. Firstly, we have characterized the binary PEG 40 monostearate/ water system, by the determination of the critical micelle concentration (CMC) value and the viscous properties. Then, the ternary phase behavior and the influence of phase structure on their macroscopic properties are studied by a combination of different techniques, namely, optical microscopy, small-angle X-ray scattering, differential scanning calorimetry and rheology. The phase behavior is complex, and some samples evolve even at long times. The single monophasic regions correspond to micellar, swollen lamellar, and lamellar gel phases. The existence of extended areas of phase coexistence (hexagonal, cubic and lamellar liquid crystalline phases) may be a consequence of the low miscibility of S40P in the lecithin bilayer, as well as, of the segregation of the phospholipid polydisperse hydrophobic chains. The presence of the PEG 40 monostearate has less effect in the transformation to the cubic phase for lecithin than that found in other systems with simple glycerol-based lipids.

INTRODUCTION

Phospholipids and fatty acids are models to mimic the biological membranes because of the formation of lamellar lyotropic liquid crystal. Lecithin is a well-tolerated and non-toxic amphiphile that constitutes the lipid matrix of many biological membranes. The phase behavior in lecithin/ water and related systems have been extensively studied by Luzzati and co-workers[1, 2]. However, until today, it is difficult to explain why solid and liquid-like chains coexist in the same bilayer over a range of temperatures. This implies differences in the thickness of different regions in the same bilayer[3]. In view of the interest of this kind of amphiphilic bilayer structure, the interactions between surfactants and fatty acids with lipids have been broadly studied.

Amphiphilic substances can be dissolved in the lipid aggregates and have the ability to destroy the lipid membranes and transform them into surfactant –lipid micelles (with surfactants) or into hexagonal and cubic phase (with fatty acids)[4]. Lipids with cationic surfactants manifest extensive swelling of the lipid's lamellar phase, with a strong dependence of lipid-surfactant electrostatic interaction effects on the lipid phase state[5], while, in the presence of non-ionic surfactants such as Triton X-100[6], there is no detectable swelling of the lamellar phase. Interaction of lipid with anionic surfactant results in a breakdown of the lamellar structures[7, 8].

In the literature, ternary phase diagrams and phase properties of systems with lecithin, water and different oils have been studied, in particular for cyclohexane[9], decane[10], isooctane[10] and

different esters derivatives of fatty acids such as isopropyl myristate[11], ethyloleate or isopropyl palmitate[12]. Those systems are of great interest due to several reasons: i) the water-rich region is an example of the effect of hydrophobic molecules on lipid bilayers, which phase transformations are involved in some biological processes as membrane fusion and budding; and ii) in the water-lean region occurs the formation of giant cylindrical reverse micelles upon the addition of small water amounts (organogels) with viscoelastic properties. Moreover, through the critical analysis of the different ternary phase diagrams, the fatty acid esters behavior is markedly different from that of hydrocarbons. In particular, in the presence of fatty acid esters there is a large portion of the phase diagram occupied by a three-phase coexistence (water, oil, and lamellar phase) instead of microemulsion such as Winsor equilibria[9, 10, 12]. The differences in the behavior have been explained by the different ability of the oils to swell the lecithin tails[12]. In addition, phosphatidylcholine/ fatty acid mixtures in water may also form inverse hexagonal and cubic phases[4]. The longer the chain length of a homologous series, the greater the preference of inverse hexagonal phase at the expense of the inverse bicontinuous cubic structure[13]. Other aqueous systems based in lecithin and biocompatible oils[14], in the presence of alcohols as emulsifiers, form microemulsions and emulsions[15-17]. The addition of alcohol decreases the rigidity of the lipid bilayer structures and leads to the formation of the microemulsion.

The interactions between lipid and polymer have also been studied[7]. The presence of polyethylene glycol (PEG) (PEG-6000 or PEG-20000) does not affect the binding of water to the choline groups of lecithin significantly[18]. In the phase diagram, 18 wt% of polymer may be solubilized easily in the lamellar phase with about 10 wt% water, and the solubility of the polymer increases upon further reduction of water content. However, other authors have reported that the presence of PEG-8000 induced dehydration of the phospholipid polar head that caused

changes in the vesicle size and form in lipid bilayers, *e.g.* dipalmitoylphosphatidylcholine (DDPC) and dimyristoylphosphatidylethanolamine (DMPE)[19]. The inclusion of phospholipids with grafted PEG chains also greatly increases the stabilization of liposomes[20]. In the case of simple glycerol-based lipids, the presence of glyceryl stearate and PEG monostearate promotes higher and faster transformation into the viscous cubic phase of glyceryl monooleate (GMO), which is used as favorite drug release matrix[21]. Moreover, the emulsifier and surface modifier properties of a series of PEG stearates favor large microemulsion regions (mainly water-in-oil) for the glyceryl monocaprate/ Tween 80/ water system[22]. This effect is more pronounced as the PEG chains get longer[22]. Microemulsions also occur in several aqueous systems with glyceryl monostearate (GMS), oleic acid (OA) or GMS/ OA as oil phases, in the presence of PEG 40 monostearate/ polyoxyethylene-b-polyoxypropylene (F68) as complex emulsifiers[23]; and for systems with glycerol monostearate (GMS) or vegetable oil using nonionic emulsifiers (F68, PEG 40 monostearate, Brij 78, soybean phosphatidylcholine and Tween 20) and ionic emulsifier (deoxycholic acid sodium, DAS)[24]. PEG 40 monostearate is considered as a non-ionic emulsifying surfactant used for the formulation of cosmetic O/W emulsions (HLB of 16.9), and it has been also used as surfactant modifiers on solid lipid nanoparticles[22-24].

Lipid-PEG bilayers are biologically friendly and physically stable. These facts are very interesting for drug delivery applications[21-24]. The advantages of using a PEG derivative are the hydrophilicity, high specificity to its target, and biological inertness to other parts of the body[25]. For all those, PEG stearates are extensively used as emulsifiers in cosmetic applications or proposed as additive in drugs carriers[21-24] but, in return, there are only few studies of the effect of PEG stearates on the phase transformation of the lipid-based formulations[22-24]. In our opinion, there is a lack of a sufficient number of comprehensive phase diagrams outlining the principles

of the lipid-polymer surfactant interactions. For this reason, in this paper, we focus on the phase behavior of the lecithin/ PEG 40 monostearate/ water system. Firstly, we have characterized the PEG 40 monostearate/ water system, by the determination of the critical micelles concentration (CMC) value and the viscous properties. Then, the pseudoternary phase behavior and the influence of phase microstructure on their macroscopic properties (optical, and calorimetrical) are studied at a constant temperature. The viscoelastic characterization of this system is of significant interest because the industrial processing for the manufacture of the commercial products with PEG stearate and/or lecithin involves the application of stress.

Materials and Methods

Sample Preparation. Soybean lecithin (Epikuron 200) was obtained from Degussa and was used without further purification. This lecithin is a mixture of phosphatidylcholines with acyl chains of different lengths and degree of unsaturation. The main component (at 68-70 wt%.) is linoleic acid, which has C-18 with two double bonds. The presence of high unsaturation (>84%) in the acyl chains brings down the melting temperature below 25 °C. The lecithin contains about 0.8 wt%. water, according to Degussa. PEG 40 monostearate, designed commercially as TEGO® Acid S 40 P (and named S40P for short in this paper) was a kind gift from Evonic Goldschmidt GmbH (Essen Germany). Its chemical structure (CH_3-$(CH_2)_{16}CO(-OCH_2CH_2)_{40}$-OH) shows that it is a hydrophobically modified PEG polymer (HM-PEG) with surfactant properties due to a hydrophobic tail of seventeen carbons (stearate) and the large hydrophilic head with forty poly(oxyethylene) groups. The presence of free ethylene oxide groups is negligible (<1 ppm).

All the samples were prepared by weighing the appropriate amounts of each component in small screw-cap vials. In order to mix the samples and remove bubbles, each mixture was centrifuged inverting the tube many times per day for several days at 4000 rpm until it was seen to be macroscopically homogeneous. If the sample could not be mixed very well at room temperature, it was heated at 65 ℃ during the homogenization process to facilitate a better mixing of the components. Once the samples were ready, they were stored in a water bath at 30.0 ± 0.1 °C. All samples are labeled in this paper as content of lecithin/ S40P (at wt%.). Water composition is determined by the remaining up to obtain 100 wt%.

Surface Tension. The surface tensions of the aqueous S40P solutions at various concentrations were determined using the ring method with a LAUDA TE-1C tensiometer. All measurements were carried out at 30.0 ± 0.1 °C, and each experiment was repeated several times and a good reproducibility was achieved.

The critical micelle concentration (CMC) value was determined as the sharp break point in the surface tension as a function of the logarithm of S40P concentration. The slope of the linear part below the CMC was determined by the method of least squares. The excess concentration Γ_2 was estimated from the Gibbs adsorption isotherm equation (Eq. 1) and the hydrophilic area per molecule at the air/water interface by equation 2.

$$\Gamma_2 = -\frac{1}{RT}\left(\frac{d\gamma}{d\ln C}\right) \qquad (1)$$

$$a = \frac{10^{20}}{N_A \Gamma_2} \qquad (2)$$

where R is the Gas constant, T is the absolute temperature, γ is the surface tension, N_A is Avogadro's number, C is the concentration of the S40P surfactant in solution, and a is the hydrophilic area per molecule expressed in nm^2/molecule.

Optical Microscopy. Birefringent textures of lyotropic liquid crystals were investigated by using a Nikon ECLIPSE 50i optical microscope equipped with crossed polarizers and a Nikon Coolpix 8400 digital camera. Lyotropic liquid crystal structures were assigned to the different samples according to the textures observed. These observations were pursued at least for two months as the aggregation state of the sample may change with time. Selected samples in the single phase regions were considered for further characterization.

SAXS. Small-Angle X-ray Scattering (SAXS) measurements were carried out using a S3-MICRO (Hecus X-ray systems GMBH Graz, Austria) coupled to a GENIX-Fox 3D X-ray source (Xenocs, Grenoble), which provides a detector focused x-ray beam with λ=0.1542 nm Cu Kα-line with more than 97% purity and less than 0.3% Kα. Transmitted scattering was detected using a PSD 50 Hecus. Temperature was controlled by means of a Peltier TCCS-3 Hecus. Because of their high viscosity, the samples were inserted between two Mylar® sheets with a 1 mm separation.

The SAXS scattering curves are shown as a function of the scattering vector modulus (Eq. 3),

$$q = \frac{4\pi}{\lambda} sin\theta/2 \quad \textbf{(3)}$$

where θ is the scattering angle. The q values with our set-up ranged from 0.08 nm^{-1} to 6.0 nm^{-1}. The system scattering vector was calibrated by measuring a standard silver behenate sample. Because of the use of a detector focused small beam (300 x 400 μm) the scattering curves are mainly smeared by the detector width. This, mainly produces a widening and distortion of the peaks without strong effects on the peak position.

Liquid crystal assignation was made primarily from peak position pattern. Lamellar structures (peak position pattern 1:2:3:4...) were further fitted to the Modified Caillé Gaussian model[26, 27] to gather complementary information about bilayer characteristics. This model comprises the use of a structure factor for a stack of lamellae and a bilayer form factor, which describes the electronic density profile as the combination of a low electronic Gausian corresponding to the methyl groups contribution and two high electron density Gausian centered at $\pm Z_H$ describing the polar heads. The correlation distance between bilayers is d, the number of correlated layers forming the stack is N and the Caillé parameter η_1 is inversely related to the elastic constants of the lamellar phase[28]. The Caillé parameter decreases as the bending and bulk elastic modulus increase, that is, a small parameter implies a rigid and ordered phase. The instrumentally smeared experimental SAXS curves were fitted to numerically smeared models for beam size and detector width effects. A least squares routine based on the Levenberg-Marquardt scheme was used[26].

Differential Scanning Calorimetry (DSC). The DSC measurements were carried out by using a DSC 6 Thermal Analysis System (Perkin-Elmer Corporation U.S.A.). 10 mg of the sample were inserted in aluminum pans for each measurement in a temperature range from 8 ºC

to 90 ºC, with a constant heating rate of 1 ºC/ min. Before each measurement, the sample was carefully set at the bottom of the pan in order to avoid bubble formation, and then kept at 8 ºC for 10 min to get uniform temperature in the system. The phase transitions temperatures and transition type were determined from the peak maximum and the shape of the calorimetric curves.

Rheology. Flow and oscillatory behavior have been measured using a Rheometer Carrimed CSL 100. Cone-plate geometry with a cone radius of 10 mm and an angle of 4:0:31 (deg:min:sec) was used. All the measurements have been done at 30 ± 0.1 ºC controlled by a Peltier system attached to the plate. A chamber was used in order to prevent the evaporation of the samples during measurement. All results showed good reproducibility in different runs and different replicates.

Flow curves were measured by applying a logarithmically spaced series of increasing stress for 2 min. The viscosity (η) was calculated as the ratio of shear stress to shear rate.

Oscillatory experiments were performed under linear viscoelastic conditions, and the angular frequency of oscillation (ω=2πf) was varied from 0.1 to 20 Hz at constant stress. In the analysis of the micellar samples, we have applied the Maxwell model. The dynamic properties of the Maxwell element (a spring and a dashpot connected in series) can be represented by linear differential equations. The solutions of these equations give the desired material functions:

$$G' = \frac{\eta \tau \omega^2}{1+\tau^2\omega^2} \qquad (4)$$

$$G'' = \frac{\eta \omega}{1+\tau^2\omega^2} \qquad (5)$$

where ω is the angular frequency, τ is the relaxation time. The storage modulus (G´) and the loss modulus (G´´) are the two components of the complex modulus G* (ratio of stress amplitude to strain amplitude) and are connected to the complex viscosity (η*) through equation 6:

$$\eta^* = \frac{\sqrt{\left[(G')^2 + (G'')^2 \right]}}{\omega} \qquad (6)$$

The Maxwell model predicts that, at high angular frequency, the storage modulus attains a plateau value while the loss modulus passes over a maximum with the angular frequency. The inverse of the frequency at which G' and G" intersect gives the value of the relaxation time.

RESULTS AND DISCUSSION

Binary S40P/ water system

PEG 40 monostearate in water forms micelles from above the critical micelle concentration (CMC) up to a value of 70 % (wt.) S40P in water. Its CMC value, obtained from surface tension corresponded to 51 μM, at 30 ºC (Fig. S1, given in Supplementary Information). From Gibbs adsorption equation (Eq. 1), the surface excess concentration was found to be $1.24 \cdot 10^{-6}$ mol/m^2, with an area per molecule of 1.4 nm^2, calculated by Eq. 2. Those values are similar to those obtained for the same system at 23 °C at the water-air interface measured by a fluorimetric method with a neutral fluorescent probe, and by a micropipet technique for interfacial tension measurements developed by the authors[29]. The relatively large area per molecule is consistent with the large PEG molecule exerting a lateral pressure and is the consequence of the large hydrophilic head with forty poly(oxyethylene) groups.

We have also studied the viscosity of the micellar samples by flow experiments. The behavior was Newtonian in all cases, with viscosity independent of the shear rate. In Fig. 1, we can see that the zero-shear rate viscosity increases strongly by increasing the S40P content up to 50% (wt.). The existence of a maximum can be attributed to the presence of a greater number of aggregates followed by their increase in size. If micelles are large enough (at the maximum) to be very flexible, the viscosity decreases. The same observation has been found in microemulsions with HM-PEG polymers[30], and for micelles in systems with surfactants[30-32].

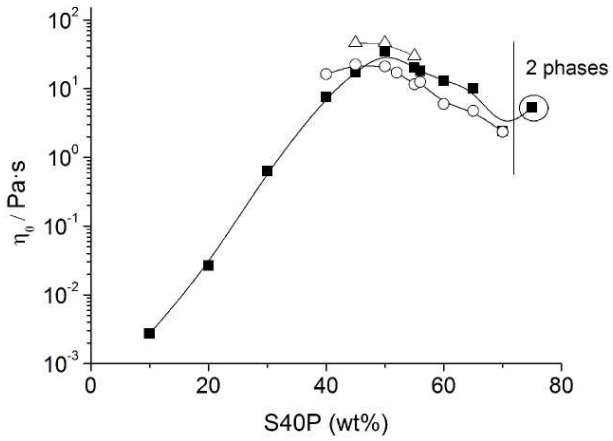

Figure 1 Logarithmic plot of zero-shear-rate viscosity as a function of the S40P content, at 30 ºC (micellar phase). Series at constant lecithin/ S40P (wt%.) ratio: (○), 0.05; (△), 0.11; and (■), binary S40P/ water system. The lines are a guide to the eye.

Ternary lecithin/ S40P/ water phase behavior.

In general, if the research wants to give a comprehensive interpretation of the system in terms of attraction/repulsion forces, free energies, or to create a theoretical model that may permit the interpretation of the phase diagram, all the components of a system should be pure. This allows

reducing and controlling the number of variables under study. We note here that we focus on a real system since lecithin and S40P are widely used in everyday life as surfactants, and/or mixtures adopted in human and animal food, medicine, cosmetic and pharmaceutics. Therefore, it is more difficult to extract scientific information from such complex phase behavior. Nevertheless, the results improve the knowledge of phase behavior of commercially applied systems.

The pseudo-ternary phase diagram of lecithin/ S40P /water system at 30 ºC, determined by a combination of different techniques such as optical microscopy with crossed polarizers, SAXS, DSC, and rheology, is given in Figure 2. Phase boundaries are delimited with error smaller than 3 wt%. The ternary system shows a fluid isotropic phase and several lamellar liquid crystalline phases, separated by multiphasic regions, where other liquid crystalline phases coexist.

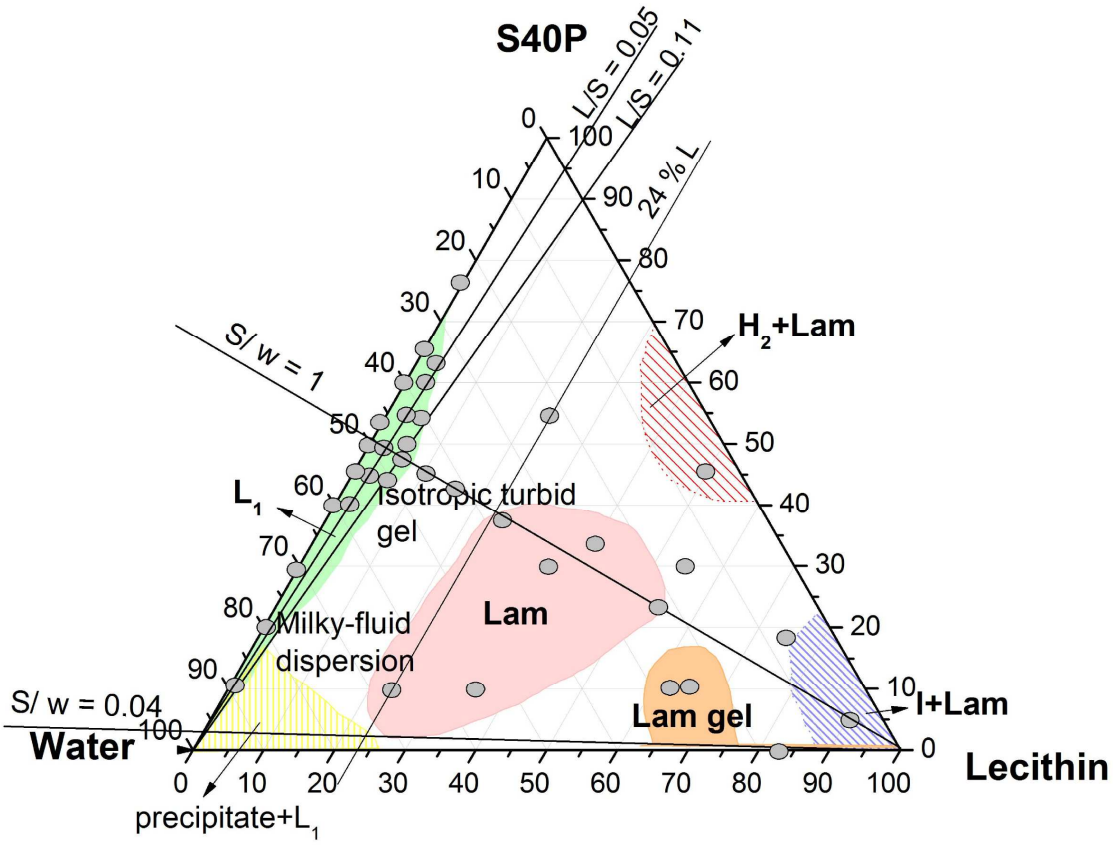

Figure 2. Phase diagram for the soybean lecithin-S40P-water system at 30℃. L_1, isotropic micellar region; Lam, lamellar phase; H_2, reverse hexagonal phase; I, inversed micellar cubic phase; S, S40P; L, lecithin; w, water. Solid lines indicate fixed ratio compositions of measured samples by different techniques. Circles correspond to the experimental points discussed in the data analysis.

The lecithin/ water system forms a lamellar phase at 63 wt % lipid. Below this lipid content, there is a biphasic region consisting of the lamellar liquid crystal dispersed in water[33]. A narrow area of micelles (L_1) is formed along the binary S40P/ water axis with the maximum uptake of about 7 wt % lecithin, at equal proportions of S40P and water (Fig. 2). This is a clear, yellowish

isotropic and fluid solution. In the water-rich corner, there is an emulsion region that separates by ageing in less than one week in two macroscopic phases: white precipitate (bottom) and isotropic solution (up). None of them was further studied in detail. With increasing S40P content, there is a region of undefined milky fluid dispersions, where lamellar domains dispersed in isotropic bulk are clearly identified by optical microscopy textures. Besides, a further increase in S40P content, between the isotropic region L_1 and the denoted lamellar region (Lam), samples have the macroscopical appearance of isotropic turbid gels. They do not show phase separation, even if the samples are centrifuged at 4000 rpm during an hour.

In the region of the phase diagram given by the composition range of 0.04 < S40P/water (wt%) < 1, which contains higher amount of water respect to the S40P, there are two different lamellar structures, according to textures by optical microscopy with crossed polarizers (Fig. 3), SAXS, and DSC studies (discussed at the following sections). A typical Maltese crosses texture of lamellar phase (Fig. 3a) is appreciated for samples of the liquid crystalline lamellar region while a "white" birefringence texture (Fig. 3b) appears for samples with more than 60 wt % lecithin content in the lamellar gel region (see also Fig. 2). The latter is similar to the texture of the lamellar gel phase of the binary lecithin/water system. In the upper-region of the phase diagram, with composition S40P / water (wt%) > 1, a typical mosaic texture of a "concentrated" lamellar phase is detected (Fig. 3c). Nevertheless, analyses with complementary techniques always detected coexistence with other phases. Because the samples were prepared with amounts that differ less than 2 wt% in composition, the single phase region must be very small. Those results are discussed in the following sections.

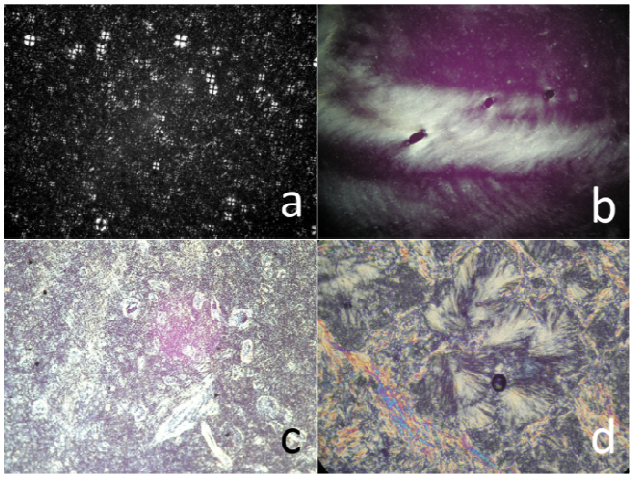

Fig. 3. Photomicrograph of the samples labeled as lecithin/ S40P (wt%): (a) 35/ 30; b) 68/ 10; c) 55/ 30; d) 75/ 18.

The maximum swelling capacity of the pure lecithin bilayer increases enormously by the addition of S40P. Even with low amounts of S40P (at 2 wt%), the bilayer swells to 80 wt% water, and the stability of the lamellar phase extends to lower lecithin content, from 63 wt% of lecithin in binary lecithin/water system to 20 wt% for the ternary system (see Fig. 2). Completely different behavior is found for the lecithin/ Triton X-100 / water system at 305K, where only an isotropic solution L_1 phase exits. It can solubilize a maximum of 10 wt% of lecithin[6]. This nonionic surfactant has shorter ethylene oxide chain (n= 9-10). In the case of lecithin/ PEG/ water systems, no significant change in the stability of the lamellar phase was detected, nor any effect on the chain length of the ethylene oxide groups[18]. Remarkably, the extent of swelling in presence of S40P is more comparable to the addition of ionic surfactants to the lecithin/ water system than other PEG or PEG-based surfactants. A low miscibility of the S40P in the lipid bilayer and a large hydration of the 40-ethylene oxide groups could favor the extent of the swelling. The different behavior could be due to the coexistence in the same molecule of an

appreciably large S40P head group and a still important hydrophobic chain, which still anchors the molecule to the bilayer.

At water content lower than ~16 wt%, the lamellar gel phase is in equilibrium with a cubic liquid crystalline phase in the proximity of the lipid corner of the phase diagram. Besides, a reverse hexagonal liquid crystalline phase (H_2) coexists in equilibrium with a "concentrated" lamellar phase and isotropic matrix, in a quite large region extending along the lecithin/ S40P axis (Fig. 3d). The area of occurrence of those monophasic liquid crystalline regions (cubic and H_2) could not be precisely delimited. Areas where optical microscopy technique shows coexistence of those phases (Lam + I; Lam + H_2) have been marked on the phase diagram (Fig. 2).

SAXS

We have studied the SAXS patterns of several compositions in the ternary phase diagram at 30 ºC. All samples are labeled as % lecithin/ % S40P, given in wt%. The measurements were performed after six months from sample preparation. All of the studied samples show the presence of lamellar phases characterized by quasi-Bragg peaks at positions 1:2:3... with respect to the beam center. Some of the samples show the coexistence of the lamellar phase with other structures at smaller q than the main peak of the bilayer. The scattering patterns have been fitted to a modified Caillé model with a bilayer electronic density model based in three Gausian; one of them describing the methyl groups and the two other describing the polar heads. The fit has been restricted to the region where the stacked bilayer is the main contribution to the scattering curves. The Scattering curves together with the fitted curves are shown in figure 4.

For samples in the lamellar region (see dots in Fig. 2), a small peak at smaller q values than that of the main peak of the lamellar phase (pointed by an arrow in the Fig. 4) is clearly identified for sample 35/ 10. The same peak could be present in the form of the broadening of the main peak also in samples 55/ 23 and 23/ 10. This could indicate the coexistence of a separated highly-swollen lamellar phase with a repeating distance of 142 Å. In our opinion, this could be more related to the sedimentation of lamellar bilayers by ageing, or segregation of domains consequence of the chain heterogeneity of the lipid[2]. Although the possibility of a P_β phase is plausible, the presence of this phase is not confirmed by the presence of WAXS peaks in the expected positions. The WAXS spectra of these samples did not show any distinct features. On the other hand, the high level of unsaturation in the lecithin chain, favor a lower chain melting temperature, which is below 25 °C.

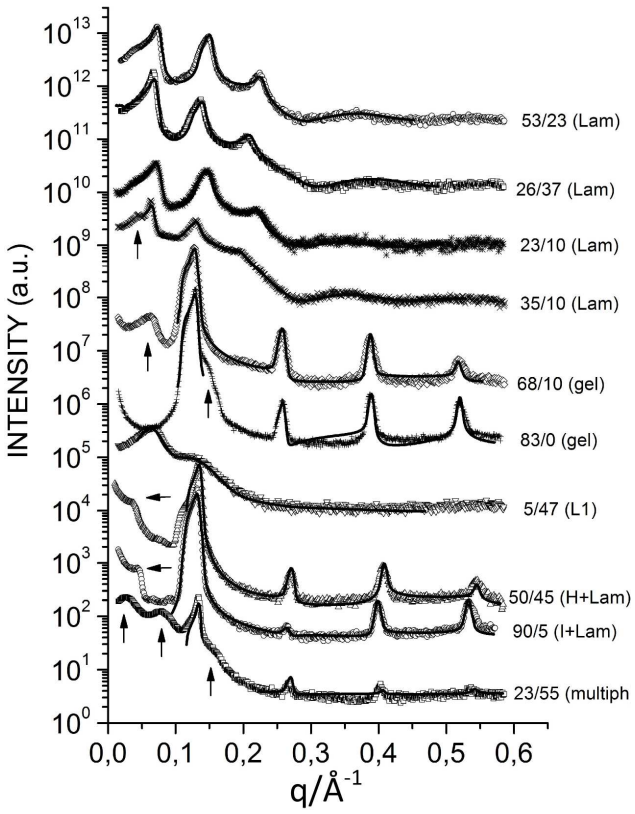

Fig 4. SAXS scans for different samples. Composition (as lecithin/ S40P, wt%.) and the corresponding phase assignation are given in the curves. Symbols: L_1, isotropic micellar region; Lam, lamellar phase; gel, lamellar gel; H_2, reverse hexagonal phase; I, inversed micellar cubic phase; multiph: multiphase region. Lines corresponds to the fitting to the Modified Caillé Gaussian model[26, 27]. The arrows correspond to specific features commented in the text.

The SAXS diffractograms for samples of composition lecithin/ S40P (wt%) of 68/ 10 and 83/ 0 (in the lamellar gel region) show several Bragg peaks corresponding to a relatively condensed lamellar structure with the same repetition distance of 49 Å (Fig. 4). They correspond to a similar composition of the bilayer, although not identical. The lamellar repeat distance results significantly shorter than the one obtained for a pure lecithin-water $L_{\beta'}$ bilayer (64 Å)[34],

therefore, the fitting of the lamellar model may indicate partial interdigitation of the bilayers. This has to be attributed to the low hydration level of the pure lecithin sample with only 17% water content because a fully hydrated bilayer seems to be achieved only for water contents above 40%. Indeed, the fitting of the curve shows the water layer to be reduced with respect to fully hydrated DPPC samples with a minor thinning also of the bilayer thickness[35]. The sample 83/ 0 was expected to be pure lamellar gel. However, the shoulder on the right of the main peak (marked by an arrow) shows the remaining of a different peak appearing short after the sample insertion in the sample holder. This peak slowly diminishes and is related to other two peaks also diminishing at relative positions $3^{½}$:$8^{½}$:$11^{½}$, which would correspond a cubic phase *Fd3m*. This reverse cubic phase is formed by inverse micelles with two different radii and is usually thought to be produced only in the presence of two differently hydrophobicity molecules, like in mixtures diglyceride/ phosphatidylcholine.[36] The sample evolves with time and, two phases with repeat distances of 57 Å and 48 Å are detected after one year (results not shown). This aging effect, as other authors proposed in different lipid structures[37], may involve the acid hydrolysis of the ester linkage present in the phospholipid chains, resulting in the formation of a fatty acid and a single-chain lipid that produce bilayer fragments.

Regarding to the sample 68 % lecithin/ 10 % S40P, in addition to the lamellar repeating distance, there is an extra band at smaller q (see the arrow in Fig. 4), which could be related to the structure of S40P in solution with the hydrocarbon chain in the melt-like state. In this case, the scattering seems to correspond to the mixture of these two structures: the water partitions between the two phases in similar proportions to that of sample 83 /0 and sample 5/ 47 (in the

micellar region). The incorporation of the S40P molecule to the system would distort the bilayer repeating distance and, therefore, change this distance and affect the peak sharpness.

Similar observations are made for the sample of composition 23 % lecithin/ 55 % S40P, where the lamellar repeat distance is a little bit shorter (46 Å), and in addition, a similar broad peak to the samples in the micellar region (5/ 47) is appreciated at q = 0.027 $Å^{-1}$ (Fig. 4). The bilayer may be dehydrated because of a favorable interaction with the PEG 40 monostearate. However, notably, the position of the maxima of the bands, signaled by arrows in Fig. 4, corresponds to 1:3:6, which, to the best of our knowledge, does not correspond to any described liquid crystalline phase.

Samples of composition of % lecithin/ % S40P contents of 90/ 5 and 50/ 45 present a scattering shoulder at lower-q values of the first Bragg lamellar peak at nearly the same position (Fig. 4). This could be indicative of structural defects of the bilayer, or of the coexistence of another type of bilayers corresponding to a repetition distance of 70 Å. Closer inspection of the pattern reveals that the first strong correlation peak and several weaker reflections can be indexed according to a body-centered structure (bcc, space group *Im*3*m* √2: √4: √6: √8: √10: √12: √14: √16*)* for a cubic liquid crystalline phase. It agrees perfectly with our observations by optical microscopy of sample 90 % lecithin/ 5 % S40P (isotropic matrix) and its calorimetrical analysis at the end of the whole temperature-up run (discussed later). Higher proportion of lamellar phase exists in the sample 90/ 5. The unambiguous identification is helped by optical microscopy inspection, where a reverse hexagonal structure is detected in the sample of composition 50/ 45, which could also be supported by the sequence of peaks at positions q of 0.039, 0.0675, 0.078 and 0.103 that correspond to the hexagonal diffraction pattern with q values

in the relationship 1: √ 3: 2: √7. Pure cubic or reversed hexagonal liquid crystalline phases have not been detected during the observation time.

The main parameters extracted from the Caillé fit to SAXS patterns (see Fig. 4) as a function of composition are given in Table 1. In case of samples with constant ratio of SP40/ water = 1 (see Fig. 2, marked by dots), both the repeating distance (d) and Caillé parameter (η_1) decrease with increasing lecithin concentrations, while the number of correlated layers (N) increases. However, the distance between the polar heads in the bilayer (Z_H) does not have a definite trend. Therefore, the addition of S40P/ water mixture to the phospholipid bilayer increases fluidity and decreases interbilayer correlation. In this series, the jump to the 90/ 5 sample is stronger because the amount of interbilayer solvent is very limited and, in addition, the coexistence with a cubic phase has been postulated above.

Table 1. Parameters of the Caillé fits of the multilayer structures corresponding to SAXS patterns of figure 4.

Sample **% Lecithin/ % S40P/ % water**	**d (Å)**	**η_1**	**N**	**Z_H**
S40P / water (wt%.)= 1				
05 /47/ 48 (L_1)	91.9	0.35	4	17.8
26/ 37/ 37 (Lam)	89.0	0.0996	18	15.0
53/ 23/ 24 (Lam)	82.7	0.083	16	15.6
90/ 5/ 5 (I+Lam)	47.0	0.0016	107	17.8

S40P = 10 wt%.				
23/ 10/ 67 (Lam)	83.9	0.10	7	16.3
35/ 10/ 55 (Lam)	93.9	0.15	53	16.1
68/ 10/ 22 (gel)	48.0	0.029	150	16.0
Lecithin ~ 24 wt%				
23/ 10/ 67 (Lam)	83.9	0.10	7	16.3
26/ 37/ 37 (Lam)	89.0	0.0996	18	15.0
23/ 55/ 22 (multph)	46.2	0.035	54	15.2
Other studied samples				
83/ 0/ 17 (gel)	48.2	0.016	28	17.5
50/ 45/ 5 (H+Lam)	47.0	0.016	14	15.4

Symbols: d, correlation distance between bilayers; η_1, Caillé parameter; N, number of correlated layers forming the stack; Z_H, correlation distance between the polar heads in the bilayer. L_1, isotropic micellar region; Lam, lamellar phase; gel, lamellar gel; H_2, reverse hexagonal phase; I, inversed micellar cubic phase; multiph: multiphase region.

For swollen lamellar samples at constant content of 10 % SP40 (samples 23/ 10 and 35/ 10, marked on figure 2), exchanging phospholipid by water does not have a strong effect on elasticity of the bilayer (η_1), although it seems to have some effect on bilayer correlation (N). The stronger effect corresponds to the change from the swollen lamellar to the rather dry lamellar gel phase (sample of composition 68 % lecithin /10 % S40P) where the Caillé parameter η_1 decreases one order of magnitude and the repetition distance halves, while the number of correlated lamellae (N) increases significantly.

At nearly constant phospholipid content (at ~24 wt%., see phase diagram in Fig. 2), the number of correlated lamellae (N) and bilayer rigidity (inversely related to the Caillé parameter

value) increase as the water is exchanged by S40P. Again, the effect on Caillé parameter is stronger when the lamellar phase becomes dry, for sample 23% lecithin/ 55 % S40P. This sample presents repetition distance corresponding to approximately half the repetition distance of the swollen samples. It is located in the multiphasic region because, in addition to the lamellar phase, present also some bands corresponding to an unknown phase, as was mentioned above.

DSC

A mapping of the phase diagram was performed to determine the phase transitions induced by temperature by differential scanning calorimetry. Thermograms were recorded with good reproducibility regarding the transition temperatures, and the presence of S40P causes decrease of the phase transitions sharpness (Fig. 5a). The thermotropic behavior of the self-assembling lipid depends on the initial phase of the sample. However, asymmetry broad peaks are observed for all samples and the different phase transitions. The nature of the structures formed after the whole up-temperature-run was identified by polarized optical microscope during the cooling process (Fig. 5b). Previously, we checked by optical microscopy that the microstructures formed in the up-temperature ramp were the same than those formed in the down-temperature ramp.

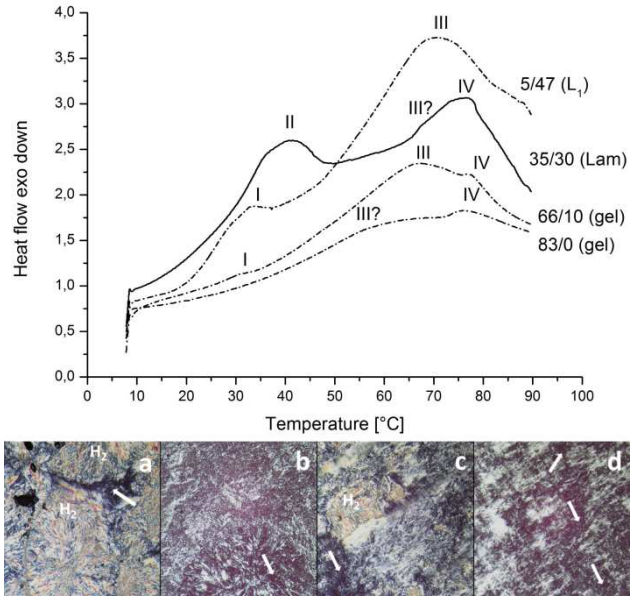

Fig. 5. Up: DSC thermograms of different samples. Composition (as lecithin/ S40P, wt%.) and the corresponding phase assignations are given in the curves. Bottom: Photomicrographs during the cooling process after the up-temperature run: (a) 35/ 30 (Lam); (b) 5/ 47 (L_1); (c) 66/ 10 (gel Lam); (d) 83 /0 (gel Lam). Arrows point isotropic cubic region and "H_2" point reverse hexagonal structure.

At 30ºC, sample 35/ 30 (given as lecithin/ S40P, wt%.) corresponds to a sample build up mainly by swollen bilayers, according to SAXS data of several samples located in the same region, such as 35/ 10; 23/ 10 or 55/ 23 (see Figs. 2 and 4). It's thermogram shows three heating endothermic transitions, which could correspond to fluid lamellar (II, aprox. 42 ºC), cubic (shoulder III, aprox. 65 ºC) and reverse hexagonal (IV, aprox. 77 ºC) phase transitions in order of increasing temperature, respectively. This could be an expected sequence in comparison to the binary soybean lecithin/ water system[1, 33]. The L_α-to-H_2 transition has been detected at 61.6 ºC for phosphatidylethanolamine[38], but in case of lecithin, a cubic structure followed by a reverse

hexagonal seems to be preferred[1]. The transition temperature value of 42 ºC (peak II) is in the same temperature range that the reported for the gel-to-fluid lamellar transition in the system 1,2-dipalmitoyl-*sn*-3-phosphocholine (DPPC)[39-41]. However, we can not assert this transition of gel (L_β or P_β)-to-fluid (L_α) lamellar bilayers because, we have not detected any gel-type bilayer by SAXS spectra either WAXS reflections for the samples in the same Lam region of the phase diagram at 30 ºC. Our experimental results agree with the high unsaturation of the acyl chains in the used lecithin (Epikuron 200) that results with a melting temperature below 25 °C. Concerning the peak at the highest temperature (IV), it should correspond to the cubic-to-reverse hexagonal phase transition according with the photomicrograph taken during the cooling process after the DSC up-temperature run (Fig. 5b, bottom). The high viscosity and the black domains in the polarized microscopy photograph could indicate the existence of the cubic liquid crystalline phase, and there is probably an overlapping of two different structures since, in addition, we detected broad peaks. In this case, there is a merging of the lamellar-cubic (III) and cubic-hexagonal (IV) transitions. Both hypotheses are reinforced by the DSC thermograms of samples in the isotropic solution phase (sample 5/ 47, Fig. 5b bottom) where there is isotropic matrix in the photomicrograph up to 70 ºC. For that sample, the peak (I) at ~33 ºC could correspond to the transition from the isotropic fluid solution to a bilayer structure. The peak (I) is sensed in the sample of composition 66 % lecithin/ 10 % S40P (in the lamellar gel region), where SAXS analysis fits better, considering the existence of S40P in solution with the gel bilayer structure. Furthermore, for sample 83% lecithin without S40P, where micelles are absent, the peak (I) is not present. The different heat flow ratio between peak (III) and (IV) for samples 66/ 10 and 83/ 0 may be due to of different proportion of the coexisting phases.

The fact that the onset transition temperature at peak (I) remains less affected with the content of S40P, and the asymmetry of broad peaks may indicate the presence of the S40P-rich and –poor domains in the bilayer, consequence of the low miscibility of the S40P in the lecithin bilayer. Similar effect is reported for other phospholipid bilayers containing ceramides.[42]

RHEOLOGY

Micellar region

Samples behave as pseudoplastic, with the exception of the samples with 3 wt% lecithin and 65% or 70% of S40P (near the phase boundary) that are Newtonian (micellar flow curves are given in the Supplementary Information as figure S2). For pseudoplastic samples, the high values of viscosity, as well as the dependence of the viscosity with shear rate, are signs that these mixed micellar aggregates in aqueous solution are elongated[32, 43, 44]. Initially, the value of viscosity, $\eta_{o,}$ is constant, due to the non-spherical aggregates distributed randomly, but above a critical shear rate ($\dot{\gamma}_c^o$) these aggregates tend to orient in the direction of flow causing a decrease in viscosity. In particular, the value of $\dot{\gamma}_c^o$ tends to decrease as the lecithin content increases. The viscosity values at zero-shear rate (η_o) for the series at constant lecithin/ S40P ratio go through a maximum by increasing the S40P content in the sample as it was clearly observed in the binary S40P/ water system, and in several viscoelastic micellar systems with surfactants (Fig. 1)[30-32]. On the other hand, the presence of lecithin has much less effect on the η_o values than the content of S40P (Fig. 1).

Lecithin in water forms bilayers. Therefore, if it is assumed that S40P micelles do not interact with the lipid bilayers, the relative viscosity of the lamellar phase ($\eta_0 / \eta_{0,dte}$) could be calculated by

dividing the viscosity value of a sample of the lecithin/ S40P/ water system by the viscosity value obtained for the "solvent" (*i.e.*, micelles of S40P in water) at the corresponding S40P composition. According to Fig. 6, there is a decrease in the relative viscosity, but starts to rise again at a content of S40P similar to that at which the binary water S40P has its maximum in viscosity (see Fig. 1). This is an indication that there are interactions between S40P and the lipid bilayer aggregates in the whole range of composition. In the absence of charges of the S40P, the nature of those interactions should be hydrophobic.

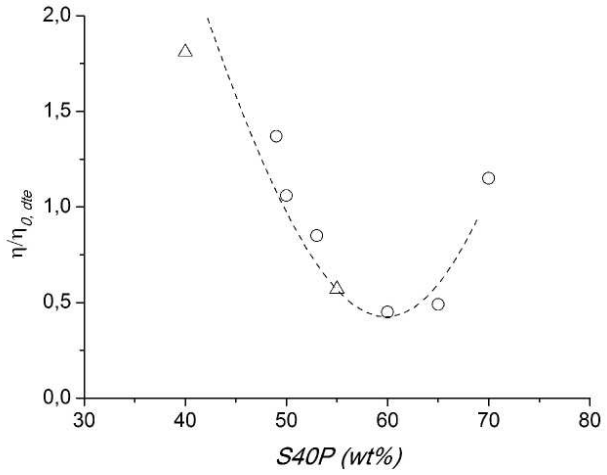

Fig. 6. Relative viscosity for series at nearly fixed ratio of S40P/ lecithin (wt%): ○, ~ 0.05; △, ~ 0.11. The line is a guide for the eye.

The viscoelastic properties of two samples with ~ 6 wt% lecithin content and different amount of S40P were also checked by using oscillatory experiments (Fig. 7). They correspond to the same lecithin/ S40P (wt%) ratio of 0.11. Their behavior can be described by the Maxwell model, with a single relaxation time τ and a single instantaneous elastic modulus G_o. The modulus of the complex viscosity is constant at the lower frequencies studied and that value agrees with the zero-shear-rate viscosity η_o obtained from the stationary flow experiment of the respective

samples (see Fig. 1). Both moduli, G' and G", increase with the angular frequency with the slopes predicted by Maxwell model: -2 and -1, respectively. Although, the Maxwell model predicts that, at high frequency, the storage modulus G' attains a *plateau* value (G_o) while the loss modulus G" passes over a maximum with the frequency, those are not obtained in our frequency observation window. Then, G' and G" were fitted simultaneously using the Maxwell equations, where the relaxation time τ and the *plateau* modulus are the only parameters of the fit. Values of relaxation times of 9.5 (± 0.5) ms and 4.8 (± 0.2) ms correspond to samples with S40P contents of 50 and 54 wt%, respectively. These values are of the same order of magnitude than viscoelastic rodlike micelles in surfactant systems[43]. Also, G_o results in values of 2.7 (± 0.2)$\cdot 10^3$ Pa and 3.7 (± 0.3)$\cdot 10^3$ Pa by increasing the S40P content, which indicates that the sample with 54 wt% of S40P is more elastic than the other one, and, in particular, its relaxation time halves the other one.

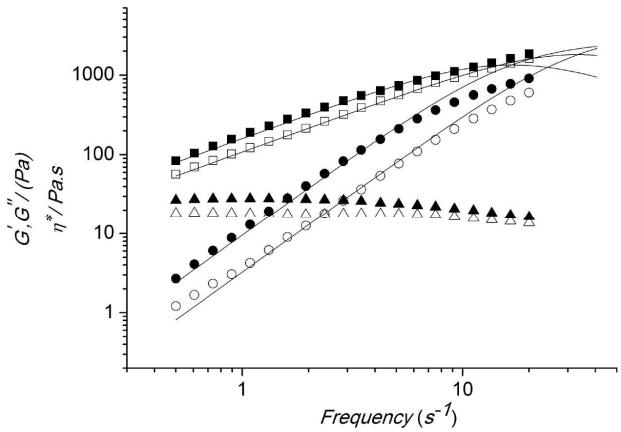

Fig. 7. Complex viscosity modulus $|\eta^*|$ (Δ), storage modulus G' (○), and loss modulus G" ( ) versus frequency of samples at mixed micellar region. Compositions of lecithin/ S40P (wt%): 6/ 54, hollow symbols; 5.5/ 50, filled symbols. Lines are the fit to the Maxwell model, with χ^2=0.00514 and χ^2=0.00759, respectively.

The zero-shear viscosity in solutions of entangled rodlike micelles is given by the product of the shear modulus and the longest structural relaxation time in the system, $\eta_o = G_o\tau$. Then, the viscosity is the result of structure and dynamic behavior through the structural relaxation time[43]. For the studied samples of composition 6/ 54 and 5.5/ 60 (lecithin/S40P, wt%.), both relaxation time and modulus of the complex viscosity decrease oppositely to S40P content in the sample. In conclusion, S40P composition affects drastically the size and stiffness of the elongated (*e.g.* rodlike) micellar aggregates, as well as their dynamic properties. From this perspective, it is likely that for the maximum of η_o curve described by the flow experiments (Fig. 1), the micelles could reach their maximum length and, with further amount of SP40 (> 50 wt%.), they could become more flexible.

Lamellar Phases

The rheological behavior of the lipotropic liquid crystalline phase is often strongly dependent on shear history; therefore, we have carried out all the experiments under the same conditions, as described in the experimental section, and without preshear-treatment. The viscosity curve of samples of composition 35 % lecithin and 30% S40P presents two power law regions separated by a region where the viscosity passes through a maximum centered at a critical shear rate, ca.120 s^{-1} (Fig. 8). The maximum might imply structural changes under shear at the critical shear rate. The high water content (35 wt%.) might produce defects in the bilayer, already before shearing, which also favors the formation of the maximum of viscosity[45]. Similar flow behavior has been detected in the lecithin/ DDAB/ water system with an associative interaction between two binary lamellar phases[45, 46], and in other lamellar liquid crystalline phases containing other

types of surfactants[45, 47]. Structural changes are related to the applied stress values but also to the time during which those stresses are applied. However, this aspect has not been studied further.

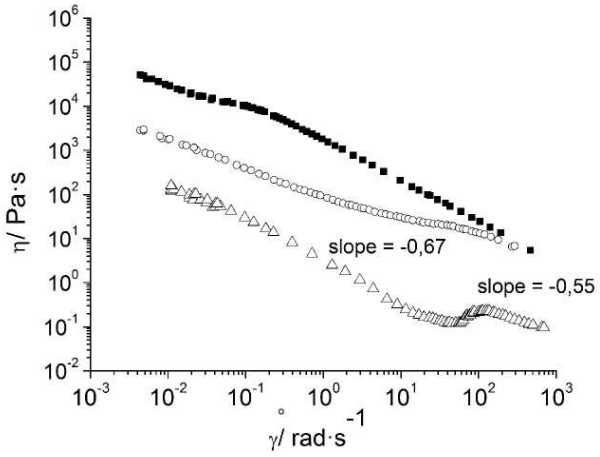

Figure 8. Viscosity as a function of shear rate for samples of composition S40P/ lecithin (wt%): △ 35/ 30 (in Lam phase); ○ 40/ 35 (in Lam phase); ■ 68/ 10 (in Lam gel phase).

For samples with lower water content (~24 wt%.), the viscosity decreases monotonically with the increase of shear rate (Figure 8). This behavior is similar to that found for open bilayer lamellar structures with lamellae oriented to the streamline or to vesicles, with a progressive increase of sizes[45, 48, 49]. The sample of the lamellar gel region has viscosity values several orders of magnitude higher than the sample in the swollen lamellar region.

The oscillatory experiments on these same samples are discussed based on the values of the loss tangent ($\tan\delta = G''/G'$), shown in Fig. 9. It indicates that all these samples are more elastic than viscous as the storage modulus (G') is higher by about one order of magnitude than the loss modulus (G") in the entire range of frequency investigated. The loss tangent is slightly frequency dependent, which results not completely parallel moduli. However, the structural relaxation time

can be considered that tends to infinity. This behavior corresponds to the so called gel behavior and is comparable to results obtained in the lamellar phases of different topologies (vesicles and stacked bilayers) of many surfactant systems[44, 50], and in particular, with lecithin[45, 46]. Samples in the lamellar region (40/ 35 and 55/ 23) have lower elasticity than samples in the lamellar gel phase (68/ 10) (i.e., the lower tanδ, the greater the elasticity). As the water content is nearly constant, the loss tangent suggests a more elastic consistency of the bilayers with increasing the lecithin concentration. On the other hand, the complex viscosity modulus decreases strongly with slopes close to -1, thus corresponding to gel behavior[51].

Although literature reports indicate the co-existence of different types of lamellar phases in mixed surfactant systems[5, 52], their rheological properties are still not very well understood. Nevertheless, some authors connect the existence of planar bilayers with a weak-like response (G" is slightly dependent on the frequency) and, even with a high-frequency crossover of G' and G", as in case of the diluted (< 43 wt% water) lecithin/ DDAB/ water system[46]. Although there are not clear evidences of the later in the lecithin/ S40P/ water system, the loss modulus is slightly frequency dependent mostly in samples of the swollen lamellar region (40/ 35 and 55/ 23) and of the lamellar gel phase (68/ 10), as is deduced from the loss tangent plot (Fig. 9). However, from the SAXS measurement, we could not assign a bilayer topology because large multilamellar vesicles are equal to flat bilayers at a local level.

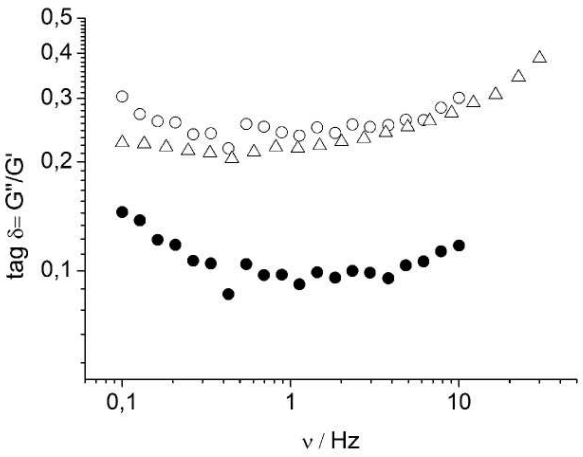

Figure 9. Loss tangent as a function of frequency for samples of composition S40P/ lecithin (wt%): △ 55/ 23 (in Lam phase); ○ 40/ 35 (in Lam phase); ■ 68/ 10 (in Lam gel phase).

CONCLUSIONS

Although PEG stearates are extensively used as emulsifiers in cosmetics, or as drug-carriers in lipid-based formulations, in the literature there is a lack of extensive studies that allow to outline the principles of the lipid-polymer surfactant interactions completely. In this work, we contribute to enlarge the existing knowledge by presenting a new phase diagram of lecithin/ PEG 40 monostearate/ water system at 30 ºC using commercially available reagents in order to approach their real life use.

The phase behavior is complex, and the single monophasic regions correspond to micellar, swollen lamellar, and lamellar gel phases. The presence of the PEG 40 monostearate has less effect in the transformation of the lecithin lamellar phase to the cubic phase than what it was found in other systems with simple glycerol-based lipids such as glyceryl monooleate[21]. Moreover, microemulsion formation might require the addition of other co-surfactants as it also occurs for simple lipid systems[22].

The calorimetric broad peak transitions, the corresponding photomicrographs at the end of the temperature-up run, and the complex SAXS profiles reflect that, over a wide composition range, several lamellar, cubic, and reverse hexagonal structures coexist. This extended phase coexistence may be a consequence of the low miscibility of S40P in the lecithin bilayer as well as of the segregation of hydrophobic chains of the phospholipid polydisperse hydrophobic chains. In addition, SAXS experiments seem to prove that, PEG 40 monostearate dehydrates the bilayer, probably due to its favorable interactions with water molecules. Rheological measurements indicate the interaction between elongated aqueous-S40P micelles and lipid aggregates. The lecithin content has less influence in the viscosity of the micellar aggregates than the S40P content. The latter affects drastically the size and stiffness of micelles, as well as their dynamic properties. Both the lamellar gel phase and the swollen lamellar phase have elasticity, which is greater for the former.

ASSOCIATED CONTENT

Supporting Information.

Figures relevant to the discussion of the cmc determination of S40P in water (Fig. S1) and viscosity of the micellar phase of the lecithin/ S40P / water systems (Fig. S2). This material is available free of charge via the Internet at http://pubs.acs.org

AUTHOR INFORMATION

Corresponding Author

*Gemma Montalvo, Departamento de Química Analítica, Química Física e Ingeniería Química. Universidad de Alcalá. E28871 Alcalá de Henares (Madrid), Spain.

Present Addresses

‡ Laboratorio de Estudios Cristalográficos. CSIC-UGR. E18100 Armilla (Granada), Spain.

Funding Sources

Financial support from MINECO CTQ2010-14897 and from MEC CTQ2007-65421/BQU

ACKNOWLEDGMENT

The authors are grateful to Professor Michael Gradzielski for contacting Evonic Goldschmidt GmbH, who supplied us the TEGO® Acid S40P reagent. Marta Rodriguez is gratefully acknowledged for preparing the samples for SAXS analysis and Jaume Caelles from the SAXS-WAXS service at IQAC for performing the measurements. Professor Pilar Tarazona is gratefully acknowledged for allowing the use of DSC equipment and Dr. Natali Fernandez for training in that technique. G. Zhang grateful for the Erasmus mobility grant, and M. Díaz grateful for her scholarship to the Agencia Española de Cooperación Internacional para el Desarrollo (AECID), Universidad de Alcalá and Banco Santander, through the "Becas Miguel de Cervantes Saavedra" Program.

This paper is dedicated to the memory of our dear Prof. Ali Khan, who was a master in phase behavior.

ABBREVIATIONS

PEG, polyethylene glycol; S40P, polyethylene glycol 40 monostearate; HM-PEG , hydrophobically modified PEG polymers; DPPC, 1,2-dipalmitoyl-*sn*-3-phosphocholine; CMC,

critical micelle concentration; SAXS, Small-Angle X-ray Scattering; DSC, Differential Scanning Calorimetry.

REFERENCES

1. Luzzati, V.; Gulik-Krzywicki, T.; Tardieu, A., Polymorphism of lecithins. *Nature* **1968** 218, 1031-4.
2. Luzzati, V.; Tardieu, A., Lipid phases: structure and structural transitions. **1974**, 79-94.
3. Tiddy, G. J. T., Surfactant-water liquid crystal phases. *Physics Reports* **1980,** 57, (1), 1-46.
4. Koynova, R.; Tenchov, B., Interactions of surfactants and fatty acids with lipids. *Curr. Opin. Colloid Interface Sci* **2001,** 6, 277-286.
5. Montalvo, G.; Khan, A., Self-Assembly of Mixed Ionic and Zwitterionic Amphiphile: Associative and Dissociative Interactions Between Lamellar Phases. *Langmuir* **2002,** 18, (22), 8330-8339.
6. Sadaghiani, A. S.; Khan, A.; Lindman, B., Liquid Crystalline of Lecithin Systems. Ternary Phase Diagrams of Lecithin-Water with Triton X-100 and Decanol. *J. Colloid Interface Sci.* **1989,** 132, 352.
7. Deo, N.; Somasundaran, P., Mechanism of mixed liposome solubilization in the presence of sodium dodecyl sulfate. *Colloids Surf. A: Physicochem. and Eng. Aspects* **2001,** 186, (1-2), 33-41.
8. de la Maza, A.; Parra, J. L., Vesicle/micelle structural transition of phospholipid bilayers and sodium dodecyl sulfate. *Langmuir* **1995,** 11, (7), 2435-41.
9. Angelico, R.; Ceglie, A.; Olsson, U.; Palazzo, G., Phase Diagram and Phase Properties of the System Lecithin-Water-Cyclohexane. *Langmuir* **2000,** 16, 2124.
10. Angelico, R.; Ceglie, A.; Colafemmina, G.; Delfine, F.; Olsson, U.; Palazzo, G., Phase behavior of the lecithin/water/isooctane and lecithin/water/decane systems. *Langmuir* **2004,** 20, (3), 619-631.
11. Harms, M.; Mackeben, S.; Müller-Goymann, C. C., Thermotropic transition structures in the ternary system lecithin/isopropyl myristate/water. *Colloids Surf. A: Physicochem and Eng Aspects* **2005,** 259, 81-87.
12. Angelico, R.; Ceglie, A.; Colafemmina, G.; Lopez, F.; Murgia, S.; Olsson, U.; Palazzo, G., Biocompatible Lecithin Organogels: Structure and Phase Equilibria. *Langmuir* **2005,** 21, 140-148.
13. Templer, R. H.; Seddon, J. M.; Warrender, N. A.; Syrykh, A.; Huang, Z.; Winter, R.; Erbes, J., Inverse bicontinuous cubic phases in 2:1 fatty acid/phosphaticylsholine mixtures. The effects of chain length, hydratation, and temperature. *J. Phys. Chem. B* **1998,** 102, 7251-7261.
14. Lei, L.; Ma, Y.; Kodali, D. R.; Liang, J.; Davis, T., Ternary phase diagram of soybean phosphatidylxholine-water-soybean oil and its application to the water degumming process. *JAOCS* **2003,** 80, (4), 383-388.
15. Papadimitriou, V.; Pispas, S.; Syriou, S.; Pournara, A.; Zournpanioti, M.; Sotiroudis, T. G.; Xenakis, A., Biocompatible microemulsions based on limonene: Formulation, structure, and applications. *Langmuir* **2008,** 24, (7), 3380-3386.

16. Leser, M. E.; van Evert, W. C.; Agterof, W. G. M., Phase behavior of lecithin-water-alcohol-triacylglycerol mixtures. *Colloid Surf. A: Physicochem. Eng. Aspects* **1996,** 116, 293-308.
17. Caboi, F.; Lazzari, P.; Pani, L.; Monduzzi, M., Effect of 1-butanol on the microstructure of lecithin/water/tripalmitin system. *Chemistry and Physics of Lipids* **2005,** 135, 147-156.
18. Khan, A.; Zhang, K.-W.; Mendonca, C., Solubilization of nonionic polymers in a lyotropic lamellar mesophase:lecithin-water-polyethylene oxyde system. *J. Colloid Interface Sci.* **1994,** 165, 253-55.
19. Bartucci, R.; Montesano, G.; Sportelli, L., Effects of poly(ethylene glycol) on neutral lipid bilayers. *Colloids Surf. A: Physicochemical and Engineering Aspects* **1996,** 115, 63-71.
20. Nikolova, A. N.; Jones, M., N., Phospholipid free thin liquid films with grafted poly(ethylene glycol)-200: formation, interaction forces and phase states. *Biochem Biophys Acta* **1998,** 1372, 237-243.
21. Shah, M. H.; Paradkar, A., Effect of HLB of additives on the properties and drug relkease from the glyceryl monooleate matrices. *Eur J Pharm Biopharm* **2007,** 67, 166-174.
22. Li, X.; Lin, X.; Zheng, L.; Yu, L.; Lv, F.; Zhang, Q.; Liu, W., Effect of poly(ethylene glycol)stearate on the phase behavior of monocarate/Tween80/water system and characterization of poly(ethylene glycol)stearate-modified solid lipid nanoparticles. *Colloids Surf.A: Physicochem Eng Aspects* **2008,** 317, 352-359.
23. Xia, Q.; Hao, X.; Lu, Y.; Xu, W.; Wei, H.; Ma, Q.; Gu, N., Production of drug-loaded lipid nanoparticles based on phase behaviors of special hot microemulsions. *Colloids Surf. A: Physicochem. and Eng. Aspects* **2008,** 313-314, 27-30.
24. Xia, Q.; Xu, D.; Lu, Y.; Xu, F.; Tang, J.; Gu, N., Preparation and characterization of drug-louded lipid nanoparticles. *J. Scientific Conference Proceedings* **2009,** 1, (2/3), 300-302.
25. Naumann, C. A.; Brooks, C. F.; Fuller, G. G.; Lehmann, T.; Rühe, J.; Knoll, W.; Kuhn, P.; Nuyken, O.; Frank, C. W., Two-Dimensional Physical Networks of Lipopolymers at the Air/Water Interface: Correlation of Molecular Structure and Surface Rheological Behavior. *Langmuir* **2001,** 17, 2801.
26. Morán, M. C.; Pinazo, A.; Clapés, P.; Infante, M. R.; Pons, R., The effect of molecular shape on the thermotropic liquid crystal behavior of monolauroylated amino acid glyceride conjugates *J. Phys. Chem. B* **2005,** 109, 22899-22908.
27. Pabst, G.; Rappolt, M.; Amenitsch, H.; Laggner, P., Structural information from multilamellar liposomes at full hydration: full q-range fitting with high-quality X-ray data. *Phys. Rev. E* **2000,** 62, 4000 - 4009.
28. Nallet, F.; Laversanne, R.; Roux, D., Modelling X-ray or neutron scattering spectra of lyotropic lamellar phases: interplay between form and structure factors. *J. Phys. II France* **1993,** 3, 487-502.
29. Lee, S. C.; Kim, D. H.; Needham, D., Equilibrium and Dynamic Interfacial Tension Measurements at Microscopic Interfaces Using a Micropipet Technique. 1. A New Method for Determination of Interfacial Tension *Langmuir* **2001,** 17, 5537-5543.
30. Karlsson, L.; Nilsson, S.; Thuresson, K., Rheology of an aqueous solution of an end-capped poly(ethylene glycol) polymer at high concentration. *Colloid & Polymer Science* **1999,** 277, 798-804.
31. Antunes, F.; Thuresson, K.; Lindman, B.; Miguel, M. G., A rheological investigation of the association between a non-ionic microemulsion and hydrophobically modified PEG.

Influence of polymer architecture. *Colloids Surf. A: Physicochem Eng Aspects* **2003,** 215, 87-100.
32. Montalvo, G.; Rodenas, E.; Valiente, M., Effects of Cetylpyridinium Chloride on Phase and Rheological Behavior of the Diluted $C_{12}E_4$/Benzyl Alcohol/Water Sytem. *J. Colloid Interface Sci.* **2000,** 227, 171-175.
33. Bergenståhl, B.; Fontell, K., Phase Equilibria in the System Soybean Lecithin/Water. *Prog. Colloid Polym. Sci.* **1983,** 68, 48.
34. Small, D. M., *Handbook of Lipid Researc: The Physical Chemistry of Lipids: From Alkanes to Phospholipids*. Second Edition, 1988 ed.; Plenum Press: New York, 1986; Vol. 4, p 672.
35. Sun, W. J.; Suter, R. M.; Knewtson, M. A.; Worthington, C. R.; Tristram-Nagle, S.; Zhang, R.; Nagle, J. F., *Phys. Rev. E* **1994,** 49, 46665.
36. Seddon, J. M., An inverse face-centred cubic phase formed by diacylglycerol-phosphatidylcholine mixtures. *Biochemistry* **1990,** 29, 7997-8002.
37. Baciu, M.; Sebai, S. C.; Ces, O.; Mulet, X.; Clark, J. A.; Shearman, G. S.; Law, R. V.; Templer, R. H.; Plisson, C.; Parker, C. A.; Gee, A., Degradative transport of cationic amphiphilic drugs across phospholipid bilayers. *Phil. Trans. R. Soc. A* **2006,** 364, 2597-2614.
38. Rappolt, M.; Hodzic, A.; Sartori, B.; Ollivon, M.; Laggner, P., Conformational and hydrational properties during the L_β–to-L_α -to H_{II}-phase transition in phosphatidylethanolamine. *Chemistry and Physics of Lipids* **2008,** 154, 46-55.
39. Urbán, E.; Bóta, A.; Kocsis, B.; Lohner, K., Distortion of the lamellar arrangement of phopspholipids by deep rough mutant lipopolysaccharide from Salmonella Minnesota. *J. Thermal. Anal. Cal.* **2005,** 82, 463-469.
40. Oszlànczi, A.; Bóta, A.; Czabai, G.; Klumpp, E., Structural and calorimetrical studies of the effect of different aminoglucosides on DPPC liposomes. *Colloids Surf. B: Biointerfaces* **2009,** 69, 116-121.
41. Kusube, M.; Matsuki, H.; Kaneshina, S., Thermotropic and barotropic phase transitions of N-methylated dipalmitoylphosphatidylethanolamine bilayers. *Biochem. Biophys. Acta* **2005,** 1668, 25-32.
42. Sot, J.; Aranda, F. J.; Collado, M.-I.; Goñi, F. M.; Alonso, A., Different effects of long- and short-cchain ceramides on the gel-fluid and lamellar-hexagonal transitions of phospholipids: A calorimetric, NMR, and X-Ray Diffraction Study *Biophysical J.* **2005,** 88, 3368-80.
43. Hoffmann, H. In *In Structure and Flow in Surfactant Solutions*, ACS Symp. Serv., Washington, DC., 1994; Herb, C. A.; Prudhomme, R., Eds. American Chemical Society Washington, DC., 1994; pp 2-31.
44. Montalvo, G.; Valiente, M.; Rodenas, E., Rheological Properties of the L Phase and the Hexagonal, Lamellar, and Cubic Liquid Crystals of the CTAB/ Benzyl Alcohol/ WAter System. *Langmuir* **1996,** 12, (21), 5202-5208.
45. Montalvo, G.; Valiente, M.; Khan, A., Shear-Induced Topology Changes in Liquid Crystals of the Soybean Lecithin/DDAB/Water System. *Langmuir* **2007,** 23, 10518-10524.
46. Youssry, M.; Coppola, L.; Nicotera, I.; Moran, C., Swollen and collapsed lyotropic lamellar rheology. *J. Colloid Interface Sci.* **2008,** 321, (2), 459-467.
47. Läuger, J.; Weigel, R.; Berger, K.; Hiltrop, K.; Richtering, W., Rheo-small-Angle-Light-Scattering Investigation of Shear-Induced Structural Changes in a Lyotropic Lamellar Phase. *J. Colloid Interface Sci.* **1996,** 181, (2), 521-526.

48. Bergmeier, M.; Gradzielski, M.; Hoffmann, H.; Mortensen, K., Behavior of a Charged Vesicle System under the Influence of a Shear Gradient: A Microstructural Study. *J. Phys. Chem. B* **1998,** 102, (16), 2837-2840.
49. Robles-Vasquez, O.; Corona-Galvan, S.; Soltero, J. F. A.; Puig, J. E.; Tripodi, S. B.; Valles, E.; Manero, O., Rheology of Lyotropic Liquid Crystals of Aerosol OT: II. High Concentration Regime. *J. Colloid Interface Sci.* **1993,** 160, (1), 65-71.
50. Abdel-Rahem, R.; Gradzielski, M.; Hoffmann, H., A novel viscoelastic system from a cationic surfactant and a hydrophobic counterion. *J.Colloid Interface Sci.* **2005,** 288, (2), 570-582.
51. Te Nijenhuis, K., *Thermorevesible Networks: Viscoelastic Properties and Structure of Gels*. Springer Verlag: Berlin, 1997.
52. Stubenrauch, C.; Burauer, S.; Strey, R.; Schmidt, C., A new approach to lamellar phases (Lα) in water - non-ionic surfactant systems. *Liq. Cryst.* **2004,** 31, (1), 39-53.

SUPPLEMENTARY INFORMATION

FIGURE CAPTION IN SUPPLEMENTARY INFORMATION

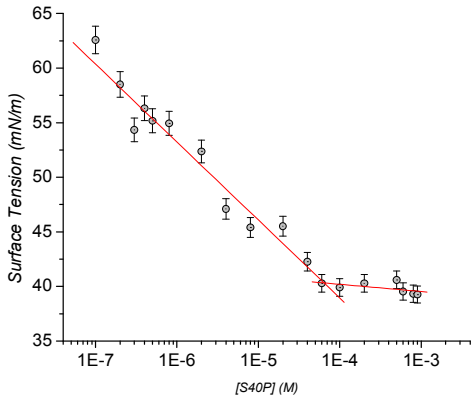

FIGURE S1. Surface tension vs. concentration of PEG-40-Stearate in aqueous solution at 30 °C at the water-air interface measured by ring method by a Tensiometer

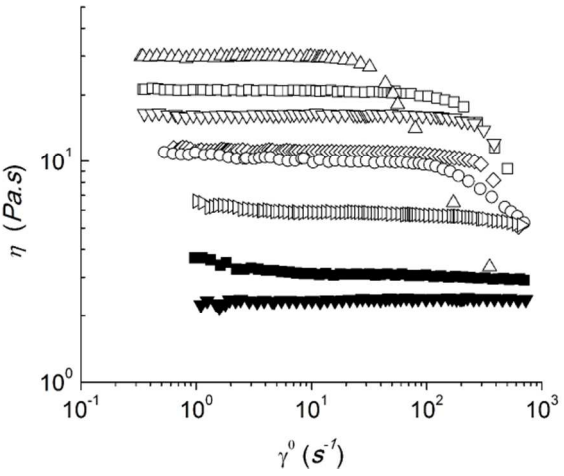

FIGURE S2. Viscosity as a function of the shear rate for samples at the isotropic fluid region, with different composition of lecithin/ S40P (wt%.), from down to up: (▼), 3.0 / 70; (■), 3.0 / 65; (▷), 3.5/ 60; (○), 5.5/ 50; (◇), 2.8/ 53; (▽), 2.0/ 40; (□), 2.5/ 50; (△), 6.0/ 54.